(Preprint) AAS 09-440

MEAN ELEMENT PROPAGATIONS USING NUMERICAL AVERAGING

Todd A. Ely*

The long-term evolution characteristics (and stability) of an orbit are best characterized using a mean element propagation of the perturbed two body variational equations of motion. The averaging process eliminates short period terms leaving only secular and long period effects. In this study, a non-traditional approach is taken that averages the variational equations using adaptive numerical techniques and then numerically integrating the resulting EOMs. Doing this avoids the Fourier series expansions and truncations required by the traditional analytic methods. The resultant numerical techniques can be easily adapted to propagations at most solar system bodies.

INTRODUCTION

The mathematical basis of perturbed, two-body mean element orbits is the averaging theory of nonlinear dynamical systems. Via averaging, short period terms (those with periods less than an orbital period) are eliminated from the variational equations of motion (EOMs) leaving only secular and long period effects. These terms define the long-term evolution characteristics of the orbit. They are ideal for orbit design and constellation design because they yield the mean characteristics useful for determining coverage and control. Also the stability characteristics of an orbit are determined via the secular and long period effects (including the possibility of chaotic motions); hence mean element trajectories are necessary for effective orbital stability studies including determination of whether an orbit meets its allocated planetary protection requirements. From a practical point of view, mean element propagations are typically one or more order(s) of magnitude faster than propagations of the full equations that include the short period terms (a.k.a., osculating elements). This speed enables mission designers to effectively explore larger design spaces to arrive at better orbit solutions for their particular mission.

AVERAGING THE EOMS

The application of averaging theory to yield mean orbital element propagations has a long history in astrodynamics with roots in the non-linear dynamical systems theory developed by Poincaré in the late 1800's. More recently, the development of the Draper Semi-Analytic Satellite Theory by Cefola [1], [2] and McClain [3], [4], [5], represents the state of the art as it has been applied to the Earth. A similar development by Kwok [6], [7] applied the theory to Mars and Venus (in addition to the Earth) and produced the POLOP software package at the Jet Propulsion Laboratory (JPL). These theories and tools applied traditional techniques that expand the EOMs

* Principal Engineer; Guidance, Navigation, and Control Section, Jet Propulsion Laboratory, California Institute of Technology, MS 301-121, 4800 Oak Grove Drive, Pasadena, CA, 91109-8099; Todd.A.Ely@jpl.nasa.gov, 818-393-1744.

in a Fourier series and analytically average the short period terms which can then be numerically propagated (hence the term semi-analytic). This approach requires the theory to derive detailed expansions for each acceleration type. A difficult task that usually requires some form of truncation (typically in eccentricity) to make the problem tractable, hence limiting the utility for highly-eccentric orbits. Furthermore, orbits around non-traditional bodies like asteroids with gravity fields that are better modeled with ellipsoidal or polyhedral formulations currently do not have analytic expressions for the averaged gravity field. In this study, the approach taken is to numerically average the variational equations and then numerically integrate the resulting EOMs. Doing this avoids the Fourier series expansion and truncations required by the analytic methods. This technique has been applied in the past by Uphoff [8], [9], and McClain [5], however they limited their investigations to fixed-order numerical averaging (typically some form of Gaussian quadrature). The present study employs modern numerical cubature routines (CUBPACK [10, 11]) to average adaptively, in addition to the fixed-order Gaussian technique. The result is a numerical algorithm that is more flexible and accurate than with the fixed order methods. Furthermore, the software package being developed (Morbiter) is designed to operate at any solar system body (rather than being fixed to the Earth, Mars, Venus), thus extending the domain of this type of analysis to anywhere in the solar system.

1ST-ORDER AVERAGING AND NUMERICAL TECHNIQUES

The trajectory of a satellite in two-body perturbed motion can be modeled in a variation of parameter formulation of 6 1st-order differential equations of motion. In its simplest form with only one fast angle and no resonances (the case of additional 'fast' angles and resonances will be examined later), these EOMs can be represented as,

$$\begin{bmatrix} \dot{\boldsymbol{\alpha}} \\ \dot{\lambda} \end{bmatrix} = \begin{bmatrix} 0 \\ n(a) \end{bmatrix} + \varepsilon \begin{bmatrix} \mathbf{f}^{\alpha}(\boldsymbol{\alpha}, \lambda) \\ f^{\lambda}(\boldsymbol{\alpha}, \lambda) \end{bmatrix}, \tag{1}$$

where the osculating elements have been selected to be an equinoctial set with $\mathbf{x} \equiv \{\boldsymbol{\alpha}, \lambda\}$, $\boldsymbol{\alpha} \equiv \{a, h, p, q, r\}$ (see the appendix for a definition of the elements), and $n(a) = \sqrt{\mu / a^3}$ is the Keplerian mean motion. Also, for convenience in later developments, set $\mathbf{f} \equiv \{\mathbf{f}^{\alpha}, f^{\lambda}\}$. The mean longitude λ has been singled out because it is the short periodic ('fast') angle in this problem. Following McClain's development [5], there exists a near-identity transformation that eliminates the mean longitude via averaging and approximates the original system in Eq. (1) to first order $O(\varepsilon)$ on time scales of order $O(1/\varepsilon)$ with a set of averaged equations of motion that take the form,

$$\begin{bmatrix} \dot{\bar{\boldsymbol{\alpha}}} \\ \dot{\bar{\lambda}} \end{bmatrix} = \begin{bmatrix} 0 \\ \bar{n}(\bar{a}) \end{bmatrix} + \varepsilon \begin{bmatrix} \bar{\mathbf{f}}^{\alpha}(\bar{\boldsymbol{\alpha}}) \\ \bar{f}^{\lambda}(\bar{\boldsymbol{\alpha}}) \end{bmatrix} + O(\varepsilon^2), \tag{2}$$

where the overbar represents the mean elements $\{\bar{\boldsymbol{\alpha}}, \bar{\lambda}\}$ and the mean perturbing functions $\bar{\mathbf{f}}(\boldsymbol{\alpha})$ and $\bar{n}^1(\boldsymbol{\alpha})$. These are obtained via,

$$\overline{\mathbf{f}}^{\alpha}\left(\overline{\boldsymbol{\alpha}}\right) \equiv \frac{1}{2\pi}\int_{-\pi+\lambda_o}^{\pi+\lambda_o} \mathbf{f}^{\alpha}\left(\overline{\boldsymbol{\alpha}},\lambda\right) d\lambda,$$
$$\overline{n} \equiv n\left(\overline{a}\right), \quad \overline{f}^{\lambda}\left(\overline{\boldsymbol{\alpha}}\right) \equiv \frac{1}{2\pi}\int_{-\pi+\lambda_o}^{\pi+\lambda_o} f^{\lambda}\left(\overline{\boldsymbol{\alpha}},\lambda\right) d\lambda \tag{3}$$

Typically the perturbation functions $\mathbf{f}\left(\boldsymbol{\alpha},\lambda\right)$ can be expanded in a Fourier series to separate secular, short period, and long period effects. This can be represented formally as,

$$\mathbf{f}\left(\boldsymbol{\alpha},\lambda\right) = \overline{\mathbf{f}}\left(\boldsymbol{\alpha}\right) + \sum_{q=-\infty, q\neq 0}^{\infty} \mathbf{f}_q\left(\boldsymbol{\alpha}\right) e^{iq\lambda}, \tag{4}$$

where performing the averaging operation identified in Eq. (3) on Eq. (4) reveals the averaged equations of motion arise from the first term in the series. Traditionally, the Fourier series is obtained via explicit manipulations of $\mathbf{f}\left(\boldsymbol{\alpha},\lambda\right)$ to arrive at analytic formulae which can be easily averaged. In the present study, the numerical average in Eq. (3) will be performed via numerical quadrature (or cubature in the multivariate case).

The motivation for considering a numerical averaging approach stems from several reasons. Foremost, any analytic theory requires some form of truncation typically in the eccentricity functions which limit the range of orbits that can be considered. A numerical averaging approach makes no such truncation. An analytic theory requires that explicit formulation of the Fourier series expansion exist in order to perform the averaging, this is not a requirement with the numerical averaging. Generalized averaging theory requires only that Eq. (1) satisfy some continuity conditions, including a Lipschitz condition, for an averaging operator to exist and to have an averaged system to be asymptotically near the un-averaged system.[12] This result is useful when considering orbital regimes where either an analytic theory hasn't been developed yet; or a convergent Fourier series might not exist for the perturbation environment. An example of this is the case of small bodies with irregular shape; mean element analytic theories haven't been developed yet, and may not exist. Finally, since the numerical approach is simpler algorithmically it represents an approach that can be implemented and tested in software more efficiently, and because of its simplicity should be easier to extend to new problem domains.

This study examines two specific numerical quadrature (cubature) techniques a classic fixed-order Gaussian method and a more recent algorithm using globally adaptive techniques developed by Genz and Cools [10] called CUBPACK. The generic cubature problem of numerically evaluating an integral can be expressed as,

$$I\left[\mathbf{f}\right] = \int_T \mathbf{f}(\mathbf{y};\boldsymbol{\alpha}) dT \tag{5}$$

where $\mathbf{y}$ is a *m*-vector, $\boldsymbol{\alpha}$ is a *r*-vector of parameters, $\mathbf{f}$ is a *n*-vector and T is a collection of *l* *m*-simplices. For the perturbed orbit problems considered here, $\mathbf{y}$ is either 1 or 2 dimensional depending on the variables that are to be averaged, $\boldsymbol{\alpha} \equiv \left\{a, h, p, q, r\right\}$, $\mathbf{f}$ is a 6-vector, and the simplices are either a line segment for single variable integration or two contiguous triangle regions (equivalent to a square) for 2-vector integration. An overview of various numerical integration techniques are described in Smyth [13] and includes the details for fixed-order Gaussian quadrature. In the current research, the integration order can be specified to be any desired integer –

typically selections range from 24 to 128. Genz and Cools [10] describe the CUBPACK algorithm as 'based on a subdivision strategy that chooses for subdivision at each stage the subregion (of the input simplices) with the largest estimated error. This subregion is divided into two, three or four equal volume subregions by cutting selected edges. These edges are selected using information about the smoothness of the integrands in the edge directions. The algorithm allows a choice from several embedded cubature rule sequences for approximate integration and error estimation.'

TWO-PERTURBED NUMERICAL MEAN ELEMENT THEORY AND RESULTS

There exist two main variation of parameter approaches used in orbit theory – Lagrange equations and Gauss' equations. The Lagrangian approach requires the system to be derivable from a potential, hence only applies to conservative force fields. On the other hand, Gauss' equations work directly with the acceleration expressions and apply to any perturbative force – conservative and non-conservative. The Gaussian approach also allows one to use the osculating accelerations directly when performing the numerical averages. This advantage allows for the re-use of a preexisting osculating elements astrodynamics software system as the basis for developing a mean element propagation capability. This research effort has done this via using JPL's Monte astrodynamics toolkit to develop a prototype numerical mean average propagation software tool, called Morbiter. Monte's API consists of compiled C++ classes and modules that can be interfaced using the Python language. Morbiter is a package of Python scripts that implement the algorithms described here, and utilizes Monte for basic astrodynamics constructs and functions such as trajectories, ephemerides, coordinate systems, astrodynamics constants, and, in most cases, the perturbation acceleration methods. Python is an interpreted language that provides an ideal platform for rapid development of algorithms, however there is a performance penalty for using Python script-based applications. In the present study, this penalty factor was about 29X in CPU time relative to a future fully compiled version of Morbiter. JPL's institutional plan is to replace the prototype software with a fully compiled version; this development is schedule to begin in the 2010 fiscal year.

Gauss' Variation of Parameters

Gauss' variation of parameter equations can be represented as,

$$\begin{bmatrix} \dot{\boldsymbol{\alpha}} \\ \dot{\lambda} \end{bmatrix} = \begin{bmatrix} 0 \\ n(a) \end{bmatrix} + \begin{bmatrix} \dfrac{\partial \boldsymbol{\alpha}}{\partial \dot{\mathbf{r}}} \bullet \sum_{j \in \mathrm{P}} \delta \ddot{\mathbf{r}}^{j} \\ \dfrac{\partial \lambda}{\partial \dot{\mathbf{r}}} \bullet \sum_{j \in \mathrm{P}} \delta \ddot{\mathbf{r}}^{j} \end{bmatrix} \tag{6}$$

where $\dot{\mathbf{r}}$ is the velocity vector between the satellite and the central body, $\delta \ddot{\mathbf{r}}^{j}$ are the perturbing accelerations. All quantities are expressed in a common inertial coordinate frame. For this study the set $P = \{Z, T, O, D, S\}$ of perturbing that will be considered are:

1. Zonal harmonics (Z),
2. Tesseral harmonics (T),
3. Other body accelerations (O),
4. Drag on a sphere in an exponentially correlated atmospheric density (D),
5. Solar radiation pressure on a sphere from the Sun (S).

The first bracket in Eq. (6) is $O(1)$ and the second term is $O(\varepsilon)$ where the small parameter ε is dependent on the specific perturbation. For instance with zonal harmonics the small parameters are the zonal harmonic coefficients J_n while for the other body perturbations it is the ratio of the satellite's semi-major axis to the other body's apparent semi-major axis around the central body a/a^O. The partials in Eq. (6) have been obtained by many authors for the equinoctial elements, c.f. Danielson [14]. For convenience, they are repeated in the appendix. Each of the perturbations in the set *P* will require a slightly different treatment, even with the numerical averaging technique.

Zonal Harmonic Perturbations

The non-spherical axial symmetric gravity acceleration perturbations (i.e., the zonal harmonics) from a central body can be expressed as the gradient of the following potential,

$$\delta\ddot{\mathbf{r}}^Z = -\nabla \frac{\mu}{r} \sum_{n=2}^{\infty} \frac{R_e^n}{r^n} J_n P_{n0}(\sin\phi) \tag{7}$$

where $\{r, \phi, L\}$ are the planet-centric spherical coordinates of {radial distance, latitude, and East longitude}, R_e is the central body's equatorial radius, $P_{nm}(\sin\phi)$ are the associated Legendre polynomials which for the zonals $m \equiv 0$, $\{J_n\}$ are the unnormalized zonal harmonic coefficients. For numerical averaging the key observation of Eq. (7) is the acceleration is dependent only on the spacecraft state $\mathbf{x}$ and not other variables, such as the orientation of the central body (as will be the case with the tesseral harmonics). That is, Gauss' equations with only the zonal harmonic accelerations take the functional form,

$$\begin{bmatrix} \dot{\boldsymbol{\alpha}} \\ \dot{\lambda} \end{bmatrix} = \begin{bmatrix} 0 \\ n(a) \end{bmatrix} + \begin{bmatrix} \dfrac{\partial \boldsymbol{\alpha}(\mathbf{x})}{\partial \dot{\mathbf{r}}} \bullet \delta\ddot{\mathbf{r}}^Z(\mathbf{x}) \\ \dfrac{\partial \lambda(\mathbf{x})}{\partial \dot{\mathbf{r}}} \bullet \delta\ddot{\mathbf{r}}^Z(\mathbf{x}) \end{bmatrix}, \tag{8}$$

which is an autonomous system that conforms to the basic averaging result identified in Eqs. (2) and (3).

Example: Consider a low altitude lunar orbiter with initial osculating orbital elements indicated in Table 1 below.

Table 1: Initial Conditions and Parameters for Frozen Low Lunar Orbiter Example

$\{a, e, i, \Omega, \omega, M\}$	{ 1858 km, 0.043, 89.4°, 0°, 270°, 0°}
Epoch	January 1, 2000 00:00:00 ET
Duration	3 years
$\{J_2, ..., J_{20}\}$	LP150Q gravity field
μ	4902.801076 km^3/sec^2
Frames	IAU Moon Pole and Fixed

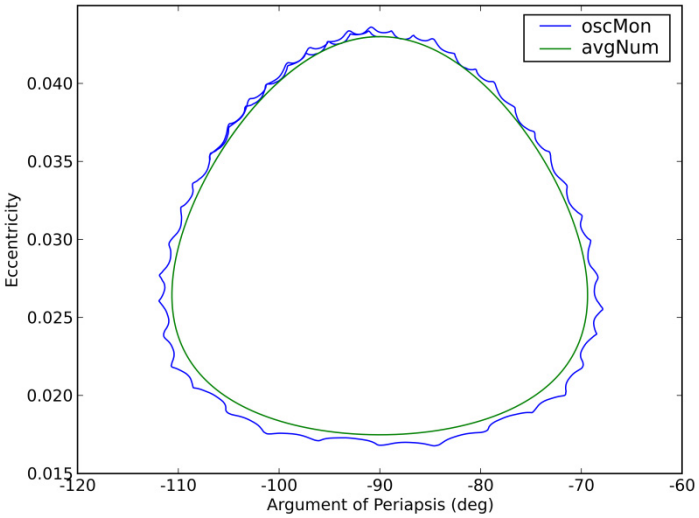

Figure 1: Argument of periapsis and eccentricity phase space of lunar orbiter.

This example is motivating because the existing mean element tools known to the author DSST or JPL' POLOP do not support mean element propagations at the Moon, hence this application represents a new mission design capability that until now hasn't been available to mission analysts. The selected elements are for a low-altitude 'frozen' orbit where the argument of periapsis ω and the eccentricity e librate with respect to each other. In this early result, the only perturbations active are the lunar zonal harmonics to the 20th order. The e-ω phase space results are shown in Figure 1 for a 3-yr propagation of the numerically averaged EOMs (labeled 'avgNum') using Morbiter and the Monte propagation of the direct osculating EOMs (labeled 'oscMon'). The results clearly show the libration characteristic with a characteristic period of about ~ 2.5 years. They also demonstrate that the averaged EOMs accurately capture the qualitative motion via comparisons to the osculating results. It should be noted that both the osculating and mean propagations have been initialized with the same initial conditions. Improved comparisons can be made via transforming the osculating initial conditions to a mean set. This will be the topic of a future study.

Tabular results of the propagation performance are presented in Table 2. The results illustrate the 'potential'[*] speed enhancement of the averaged EOMs using the 64th-order Gaussian numerical quadrature and CUBPACK with relative and absolute errors set to an absolute tolerance of 1.0E-9 and a relative tolerance of 1.0E-7 over the osculating propagation. In particular, CUBPACK-based propagation requires 76 times fewer function calls then the osculating propagation. The fixed order Gaussian result is even faster, but this was only arrived at after experimentation in finding the proper order. If the order was too low (say 16) the numerical quadrature yields errors that the numerical integration routine would need to compensate for and result in a significantly longer propagation time (on the order of the osculating result). In comparison, the

[*] 'Potential' appears in quotes because of the prototype nature of Morbiter, and its use of Python scripts. Python is inherently slower than an optimized compiled code. In this particular example, the Python time/function call compared to the C++ time/function call yields a 29X speed penalty for the Python calls. Clearly, the algorithms developed here would benefit immensely from a fully optimized compiled implementation.

adaptive quadrature using CUBPACK worked well without such an investigation. This leads to a preliminary conclusion that the adaptive routines are useful for initial studies and establishing expected results. Then with careful tuning, the analyst can use fix ordered methods for parametric trade studies.

Table 2: Comparison of numerically averaged EOMs 3-yr propagation to osculating EOMs

	Mean Gauss Fixed Order 64	**Mean CUBPACK** 1.E-9/1.E-7	**Osculating Monte**
Mean Step Size (# orbital periods)	140	244	0.004
# of Function Calls	12096	49,575	6,549,598
'Potential' Speed-Improvement Factor (osculating/mean function calls)	552.8	76.3	1

Tesseral/Sectorial Harmonic Perturbations

The non-spherical non-symmetric gravity acceleration perturbations (i.e., the tesseral/sectorial harmonics) from a central body can be expressed as the gradient of the following potential,

$$\delta\ddot{\mathbf{r}}^T = \nabla \frac{\mu}{r} \sum_{n=2}^{\infty} \sum_{m=1}^{n} \frac{R_e^n}{r^n} P_{nm}\left(\sin\phi\right)\left(C_{nm}\cos\left(mL\right) + S_{nm}\sin\left(mL\right)\right) \tag{9}$$

where again $P_{nm}\left(\sin\phi\right)$ are the associated Legendre polynomials however $m \neq 0$ and $\left\{C_{nm}, S_{nm}\right\}$ are the un-normalized harmonic coefficients (note that $J_n = -C_{n0}$). Unlike the zonal harmonics, accelerations induced by the tesseral harmonics $\left(m \neq n\right)$ and sectorial harmonics $\left(m = n\right)$ are dependent on the central body's orientation relative to the satellite, in particular via its sidereal angle θ. This too can be a 'fast' variable or 'slow' depending on the selected central body. For instance the Earth's sidereal period is ~1 day while Venus' sidereal period is 243 days. The relationship between the mean longitude λ and sidereal angle θ can be made explicit by computing the Fourier expansion of Eq. (9) in equinoctial elements, which has been done by several authors including Cefola [15], McClain [4], and Danielson [14]. The current analysis can benefit by examining the Fourier series expansion in a functional form,

$$\delta\dot{\mathbf{x}}^T \equiv \begin{bmatrix} \dfrac{\partial\boldsymbol{\alpha}\left(\mathbf{x}\right)}{\partial\dot{\mathbf{r}}} \bullet \delta\ddot{\mathbf{r}}^T\left(\mathbf{x}\right) \\ \dfrac{\partial\lambda\left(\mathbf{x}\right)}{\partial\dot{\mathbf{r}}} \bullet \delta\ddot{\mathbf{r}}^T\left(\mathbf{x}\right) \end{bmatrix} = \sum_{q=-\infty}^{q=\infty} \sum_{m=0}^{l} \mathbf{f}_{qm}^T(\boldsymbol{\alpha}) e^{j(q\lambda - m\theta)}, \tag{10}$$

where the functions $\mathbf{f}_{qm}^T(\boldsymbol{\alpha})$ are often infinite expansions as well that need to be carefully truncated in an analytic averaging theory. Examination of Eq. (10) reveals the possibility of several important cases,

1. Deep resonance exists when the mean longitude rate $\dot{\lambda}$ and the sidereal rate are commensurate. That is, there exists a rational ratio of two integers Q and P that satisfy,

$$\frac{\dot{\lambda}}{\dot{\theta}} = \frac{Q}{P} \rightarrow Q:P \text{ resonance, i.e., 2:1 is a ~12 hr resonance at Earth.} \tag{11}$$

   A shallow (or near) resonance occurs when $\dot{\lambda}/\dot{\theta}$ are close to Q/P in some sense. Typically, for the resonance to be significant Q and P should be smaller integers. That is a 2:1 resonance that excites gravity harmonics of order 2 will have much more effect than on, say, a 30:1 resonance that excites the typically much smaller order 30 harmonics.

2. No resonance; such as for an orbit that is outside of a shallow resonance region, or, as is typically the case, when $\dot{\theta} \ll \dot{\lambda}$. This applies to Venus, the Moon, and often other bodies that are tidally locked in a 1:1 spin resonance. In this case the integers which satisfy Eq. (11) are too large to be significant. The conditions that need to exist to make this determination are the subject of KAM theory of nonlinear dynamical systems theory.[16]

Each of these cases will be treated separately.

Case 1: In deep resonance or shallow resonance, the commensurability of the mean motion with the planet rotation rate introduces a new slow variable that can be revealed in Eq. (10) by introducing the stroboscopic node ψ. It is defined as,

$$\psi \equiv P\lambda - Q\theta, \tag{12}$$

Using Eq. (12) a change of variables is made to Gauss' equations in Eq. (6) to yield,

$$\begin{bmatrix} \dot{\boldsymbol{\alpha}} \\ \dot{\psi} \end{bmatrix} = \begin{bmatrix} \dfrac{\partial \boldsymbol{\alpha}}{\partial \dot{\mathbf{r}}} \bullet \sum_{j \in \mathrm{P}} \delta \ddot{\mathbf{r}}^{j} \\ Pn(a) - Q\omega_{CB} + P\dfrac{\partial \lambda}{\partial \dot{\mathbf{r}}} \bullet \sum_{j \in \mathrm{P}} \delta \ddot{\mathbf{r}}^{j} \end{bmatrix}, \tag{13}$$

where, in resonance or near resonance, Q and P have been selected to satisfy the following property,

$$\dot{\psi} = P\dot{\lambda} - Q\dot{\theta} = P\left(n + \dot{\omega} + \dot{\Omega}\right) - Q\omega_{CB} = O(\varepsilon). \tag{14}$$

Now all components of the right hand side in Eq. (13) are of $O(\varepsilon)$ or higher. To affect the chage of variable in the acceleration expressions $\delta \ddot{\mathbf{r}}_j$ in Eq. (13) the following expressions prove convenient,

$$\begin{aligned} \theta(t) &= \frac{1}{Q}\psi(t) + \frac{P}{Q}\lambda(t), \\ \lambda(t) &= n(t - t_o) + \lambda_o. \end{aligned} \tag{15}$$

Converting the argument in Eq. (10) to a stroboscopic node formulation via substituting Eq. (15) into Eq. (10),

$$\arg(t) = \left(q - m\frac{P}{Q} \right) \lambda(t) - \frac{m}{Q}\psi(t) = \left(qQ - mP \right) \frac{\lambda(t)}{Q} - \frac{m}{Q}\psi(t) \tag{16}$$

Near a resonance the stroboscopic node is a slowly varying variable by the property in Eq. (14) and the mean longitude continues to be the fast variable. In a first order formulation of averaging, the node is treated as a constant, and the mean longitude is averaged using,

$$\begin{aligned} \delta\dot{\bar{\mathbf{x}}}^T &\equiv \frac{1}{2\pi N} \int_{-N\pi}^{N\pi} \sum_{q=-\infty}^{q=\infty} \sum_{m=0}^{l} \mathbf{P} \# \mathbf{f}_{qm}^T(\boldsymbol{\alpha}) \exp j \left[\left(qQ - mP \right) \frac{\lambda}{Q} - \frac{m}{Q}\psi \right] d\lambda, \\ &= \frac{1}{2\pi N} \sum_{q=-\infty}^{q=\infty} \sum_{m=0}^{l} \mathbf{P} \# \mathbf{f}_{qm}^T(\boldsymbol{\alpha}) \exp j \left[-\frac{m}{Q}\psi \right] \int_{-N\pi}^{N\pi} \exp j \left[\left(qQ - mP \right) \frac{\lambda}{Q} \right] d\lambda, \\ &= \frac{Q}{\pi N} \sum_{q=-\infty}^{q=\infty} \sum_{m=0}^{l} \mathbf{P} \# \mathbf{f}_{qm}^T(\boldsymbol{\alpha}) \exp j \left[-\frac{m}{Q}\psi \right] \frac{\sin\left[\frac{N}{Q}\pi \left(qQ - mP \right) \right]}{qQ - mP}. \end{aligned} \tag{17}$$

where the integral number N of the averaging operation is indeterminate at this point, $\mathbf{P} \equiv \{0,0,0,0,0,P\}$, and $\#$ is the element-wise product of the two vectors $\mathbf{P}$ and $\mathbf{f}_{qm}^T$.

Following McClain [4] if N is assumed to be equal to Q then the following average results,

$$\delta\dot{\bar{\mathbf{x}}}^T = \begin{cases} \frac{1}{\pi} \sum_{q=-\infty}^{\infty} \sum_{m=0}^{l} \mathbf{P} \# \mathbf{f}_{qm}^T(\boldsymbol{\alpha}) \exp j \left[-\frac{m}{Q}\psi \right], & N = Q,\ mP = qQ \\ 0, & N = Q,\ mP \neq qQ \end{cases}. \tag{18}$$

The first result in Eq. (18) illustrates that terms satisfying $mP = qQ$ are resonant long-period terms and will survive the averaging, and those terms with $mP \neq qQ$ are short periodic and will average out. Note that for the zonal terms (m = 0) only the q = 0 term survive the averaging. However for numerical averaging, having N integral periods to evaluate in the quadrature increases the cost in terms of the number of function calls required. This motivates further investigation of Eq. (17), setting N = 1 reveals the following,

(19)

$$\delta\dot{\bar{\mathbf{x}}}^T = \frac{Q}{\pi} \sum_{q=-\infty}^{q=\infty} \sum_{m=0}^{l} \mathbf{P} \# \mathbf{f}_{qm}^T(\boldsymbol{\alpha}) \exp j \left[-\frac{m}{Q}\psi \right] \frac{\sin\left[\frac{\pi}{Q} \left(qQ - mP \right) \right]}{qQ - mP}, \quad N = 1$$

Examining this result shows that some terms in the argument for sine will be fractional and survive, hence contributing short periodic terms. However, if the values for m are restricted to those values that are integral multiples of Q then long period terms are isolated (i.e., those with $q = rP$ in the 2nd row), and the short periodic terms are eliminated when m is not an integral multiple of Q (i.e. those with $q \neq rP$ in the 3rd row). This is expressed as follows,

(20)

$$\delta\dot{\bar{\mathbf{x}}}^T = \begin{cases} \dfrac{1}{\pi}\displaystyle\sum_{q=-\infty}^{q=\infty}\sum_{m=0}^{l} \mathbf{P}\#\mathbf{f}_{qm}^T(\boldsymbol{\alpha})\exp j\left[-r\psi\right], & N=1, m=rQ, q=rP \\ 0, & N=1, m=rQ, q\neq rP \end{cases}$$

The procedure for restricting $m = rQ$ is to eliminate those coefficients $\{C_{lm}, S_{lm}\}$ from the gravity field that do not satisfy the condition. For example, in a 4 x 4 gravity field and a $Q:P=2:1$ resonance (i.e., a 12 hr Earth orbiter) the C_{lm} terms retained in the field would be $\{C_{20}, C_{22}, C_{32}, C_{42}, C_{44}\}$ while the C_{lm} set to zero would be $\{C_{21}, C_{31}, C_{33}, C_{41}, C_{43}\}$. Similar results apply for the S_{lm} coefficients. This procedure of setting appropriate terms in the field to zero, and averaging over the interval $-\pi < \lambda < \pi$ yields a more efficient numerical averaging procedure.

The preceding averaging process could also be applied to a formulation that is equivalent to Eq. (16) except that now the argument includes the stroboscopic node ψ and the average is over the sidereal angle θ. The averaging process now reveals a long period result of the form,

$$\delta\dot{\bar{\mathbf{x}}}^T = \begin{cases} \dfrac{1}{\pi}\displaystyle\sum_{q=-\infty}^{\infty}\sum_{m=0}^{l} \mathbf{P}\#\mathbf{f}_{qm}^T(\boldsymbol{\alpha})\exp j\left[\frac{q}{P}\psi\right], & N=Q, mP=qQ \\ 0, & N=Q, mP\neq qQ \end{cases} . \tag{21}$$

One should note that in the limit as $q \to \infty$ the product $q\dot{\psi}$ becomes short periodic with a diminishing coefficient that *may* be negligible (assuming a convergent Fourier series where the magnitudes of the coefficients approach zero in the limit). However, as the eccentricity increases the possibility of sufficiently large terms with frequency $q\dot{\psi}$ grows and, thus, may be retained in the averaged equations; forcing the numerical integration scheme to select smaller and smaller step sizes. It is this reason that averages over λ are preferred over θ.

Case 2: In the non-resonance case no change of variables is required and Eq. (10) can be examined directly, however under the assumption $\dot{\theta} \ll \dot{\lambda}$ the sidereal angle can be considered a constant over the averaging interval (no change of variable to stroboscopic node is needed), this leads to the following result,

$$\begin{aligned} \delta\dot{\bar{\mathbf{x}}}^T &\equiv \frac{1}{2\pi}\int_{-\pi}^{\pi}\sum_{q=-\infty}^{q=\infty}\sum_{m=0}^{l}\mathbf{f}_{qm}^T(\boldsymbol{\alpha})\exp j\left[q\lambda - m\theta\right]d\lambda, \\ &= \frac{1}{2\pi}\sum_{q=-\infty}^{q=\infty}\sum_{m=0}^{l}\mathbf{f}_{qm}^T(\boldsymbol{\alpha})\exp j\left[-m\theta\right]\int_{-\pi}^{\pi}\exp j\left[q\lambda\right]d\lambda, \\ &= \frac{1}{\pi}\sum_{m=0}^{l}\mathbf{f}_{0m}^T(\boldsymbol{\alpha})\exp j\left[-m\theta\right]. \end{aligned} \tag{22}$$

With the mean longitude eliminated the numerical propagator's step size is determined by the terms with $m\omega_{CB}$ (assuming the other angular rate terms perturbing $\boldsymbol{\alpha}$ remain of $O(\varepsilon)$), and as

m increases the frequencies increase. If the coefficients of these terms $\mathbf{f}_{qm}^{T}(\boldsymbol{\alpha})$ do not diminish fast enough they could cause the numerical propagator to chose small step sizes, hence diminishing the utility of the averaging method. Clearly the presence of these frequencies depend on the order *m* of the gravity field that the analyst has included in their analysis – the higher the order the more abundant the higher frequency terms. This indicates the need to perform another average over selected terms in Eq. (22), however a more direct method is to simply limit the order of the gravity field to ensure short period terms from the sidereal rotation have been eliminated. Later examples with Venus will illustrate the procedure.

Example of Case 1: Consider a Mars orbiter that is in a 2:1 resonance with Mars' rotation rate with initial conditions and other parameters as indicated below in Table 3.

Table 3: Initial Conditions* and Parameters for Frozen Low Lunar Orbiter Example

$\{a, e, i, \Omega, \omega, M\}$	{ 12868.635 km, 0.3, 20°, 0°, 190°, 45°}
Epoch	January 1, 2000 12:00:00 ET
Duration	5 years
$\{C_2 \cdots C_{20}, S_2 \cdots S_{20}\}$	MGS75E gravity field
μ	42828.377043 km^3/sec^2
Frames	IAU 2000 Mars Pole and Fixed

For the numerical average computations the 20x20 field is restricted to include only those orders that are multiples of $Q = 2$ (the necessary step that was developed in the theory above). In this example the numerical averaging results from Morbiter (labeled 'avgNumerical') are compared to the osculating results from JPL's Monte software (labeled 'oscMonte'), and the semi-analytic averaging result from JPL's legacy POLOP software (lableled 'avgPolop'). A plot of the semi-major axis history is shown in Figure 2. Notice that the Moribter ('avgNumerical') solution lies on top of the legacy semi-analytic solution from POLOP ('avgPolop'), with no quantitative differences being self evident. This represents a validation of the numerical averaging technique relative to the legacy code. The second observation is the mean element results correctly capture the motion as defined by the osculating solution – the only apparent differences are in small short periodic motions that can be seen in Monte ('oscMonte') result.

* For this Mars application the conversion between osculating and mean initial conditions was possible using the legacy POLOP capability that can yield pseudo-mean initial conditions via removing J_2 short periodic contributions. This capability was used in this example.

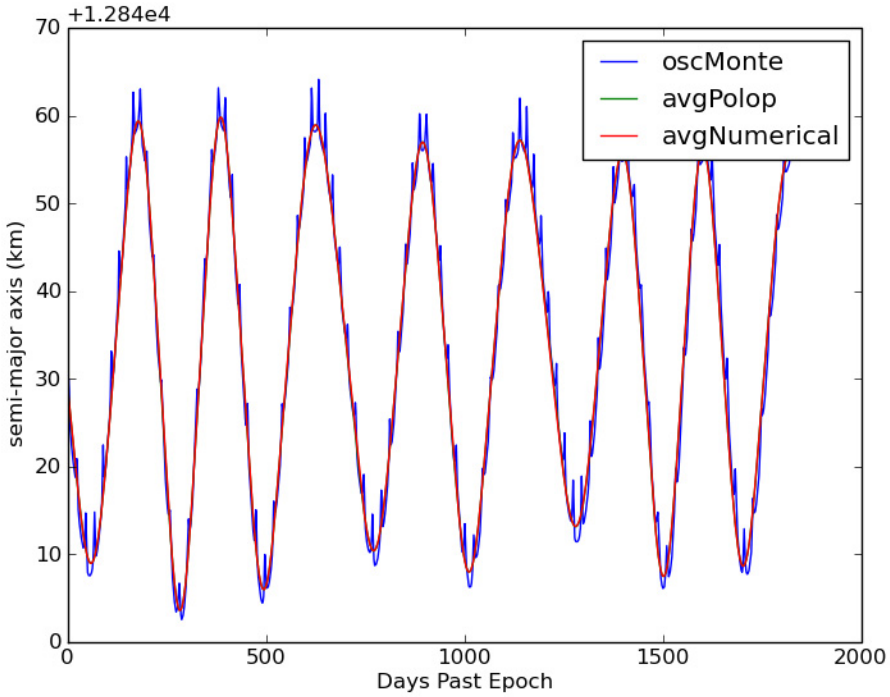

Figure 2: Semi-major axis solution for an elliptical, inclined Mars orbiter in a 2:1 resonance.

Tabular results of the propagation performance are presented in Table 4. Relative to the zonal-only results given in Table 2 the performance benefit of the averaging is not as pronounced.

Table 4: Comparison of numerically averaged EOMs 5-yr propagation to osculating EOMs

	Mean Gauss Fixed Order 64	**Mean CUBPACK** 1.E-9/1.E-7	**Osculating Monte**
Mean Step Size (# orbital periods)	4.2	4.2	0.0018
# of Function Calls	94,976	221,580	954,788
'Potential' Speed-Improvement Factor (osculating/mean function calls)	10	4.3	1

Nonetheless with an optimized compiled implementation of Morbiter the expected speed gain is on the order of 10 times. It is worthwhile comparing the execution times of the POLOP result at ~ 4.8 sec while the Monte propagation took 23.6 sec. Given the anticipated speed improvement of 10X for a future Morbiter, the numerical averaging technique would result in a 2.3 sec execution time that is over twice as fast as the semi-analytic technique.

Example of Case 2: Consider an orbiter at Venus with conditions similar to the Magellan orbiter given below in Table 5. Two scenarios are examined. In the first scenario the numerical averaging technique will include only the zonal harmonics, in the second scenario the full 10x10

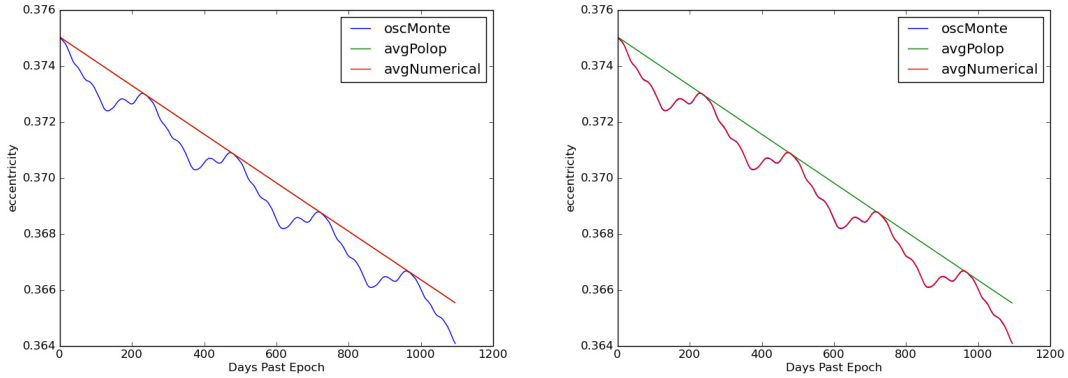

Figure 3: Eccentricity solution for a Venus orbiter. In the plot to the left the 'avgPolop' and 'avgNumerical' solutions overlay each other because the included gravity terms are 10X0 while the 'oscMonte' includes the full 10X10. In the plot the right, the 'avgNumerical' solution now includes the 10X10 field and overlays the 'oscMonte' result.

Table 5: Initial Conditions* and Parameters for Frozen Low Lunar Orbiter Example

$\{a, e, i, \Omega, \omega, M\}$	{ 10082.179 km, 0.375, 85°, 51.831°, 10.036°, 0.0°}
Epoch	July 26, 1988 00:00:00 ET
Duration	3 years
$\{C_2 \cdots C_{10}, S_2 \cdots S_{10}\}$	MGNP180U gravity field
μ	324858.77 km^3/sec^2
Frames	IAU 2000 Venus Pole and Fixed

field will be included. The osculating propagation will include the 10x10 field in both propagations. In the left plot of Figure 3; the 'avgPolop' and 'avgNumerical' solutions overlay each other because the included gravity terms are 10X0 while the 'oscMonte' includes the full 10X10. In the plot to the right, the 'avgNumerical' solution now includes the 10X10 field and overlays the 'oscMonte' result. In this example the zonals are sufficient for capturing the long term motion of the satellite. Indeed in the case of no resonance POLOP forces inclusion of only the zonal harmonics – as is the case in the two results above. Morbiter, on the other hand, provides the option to include the tesserals if the analyst so chooses. However, there is a performance penalty, the performance numbers are tabulated below in Table 6. Both numerical mean element results are

* For this Mars application the conversion between osculating and mean initial conditions was possible using the legacy POLOP capability that can yield pseudo-mean initial conditions via removing J_2 short periodic contributions. This capability was used in this example.

Table 6: Comparison of numerically averaged EOMs 5-yr propagation to osculating EOMs

	10X0 Field Numerical Mean CUBPACK 1.E-9/1.E-7	**10X10 Field Numerical Mean CUBPACK** 1.E-9/1.E-7	**10X10 Field Osculating Monte**
Mean Step Size (# orbital periods)	471	18	0.006
# of Function Calls	8,250	238,065	2,749,806
'Potential' Speed-Improvement Factor (osculating/mean function calls)	333.3	11.6	1

faster than their osculating counterpart, but, clearly, for initial trade studies the zonal-only solution yields the long term characteristics sufficiently well in a fraction of the time. Again it is worthwhile computing the potential speed of a future Morbiter compared to POLOP. Using the Monte execution speed, the time/function call can be computed and used to predict a future Morbiter performance of 0.18 seconds, which is comparable to the POLOP run at 0.24 seconds.

Other Body Perturbations

Perturbations from another celestial body can be modeled with the following,

$$\delta\ddot{\mathbf{r}}^{O} = \mu^{O}\left(\frac{\mathbf{r}^{C\to O}-\mathbf{r}}{\left|\mathbf{r}^{C\to O}-\mathbf{r}\right|^{3}}-\frac{\mathbf{r}^{C\to O}}{\left|\mathbf{r}^{C\to O}\right|^{3}}\right). \tag{23}$$

where $\mathbf{r}^{C\to O}$ is the vector from the central body to the perturbing body and μ^{O} is the gravitational constant of the perturbing body. If there are several perturbing bodies then Eq. (23) applies to each body and the total acceleration is generated via summing the individual contributors. Clearly, Eq. (23) indicates a dependency on both the state of the satellite and the other body. This introduces a time dependency that impacts the averaging process that stems from the orbital period of the other body. Typically, this period is long and the other body state can be treated as a constant over the satellite's mean longitude averaging interval. As the period reduces there is a resultant reduction in the integrator step size to accommodate the increasing frequencies present in the single averaged equations. If the frequencies get too large, a second average over the other bodies mean longitude may be warranted. The choice to do this is dependent on the specific case being analyzed. As with the tesseral harmonics, an explicit Fourier expansion in the equinoctial elements can be performed. An example of this expansion is found in McClain [4] in which the explicit dependence on both the satellite's mean longitude λ and the other body's mean longitude λ^{O} (of its apparent orbit around the central body) are revealed. Formally this expansion takes the form,

$$\delta\dot{\mathbf{x}}^{O} \equiv \begin{bmatrix} \dfrac{\partial\boldsymbol{\alpha}(\mathbf{x})}{\partial\dot{\mathbf{r}}}\bullet\delta\ddot{\mathbf{r}}^{O}(\mathbf{x}) \\ \dfrac{\partial\lambda(\mathbf{x})}{\partial\dot{\mathbf{r}}}\bullet\delta\ddot{\mathbf{r}}^{O}(\mathbf{x}) \end{bmatrix} = \sum_{q=-\infty}^{q=\infty}\sum_{t=-\infty}^{\infty}\mathbf{f}_{qt}^{O}(\boldsymbol{\alpha})e^{j(q\lambda-t\lambda^{O})}. \tag{24}$$

Compared to Eq. (10), this result is very similar and its analysis proceeds along similar lines to the tesseral harmonics. However, in the majority of cases the resonances between the satellite

mean motion and the other body's apparent mean motion are not practical because of the large disparity in mean motion magnitudes. Examination of Eq. (24) shows that there exists some combinations of $\{q,t\}$ that result in a resonance. But as either q or t increase, the coefficients $\mathbf{f}_{qt}^{O}(\boldsymbol{\alpha})$ diminish in magnitude for a convergent Fourier series. These higher resonances are not significant in most situations on time scales of order $O(1/\varepsilon)$ (again these statements can be made more precise via using the KAM theorem). Thus, it is practical to first consider the case of non-resonance, which is equivalent to the analysis performed for Case 2 of the tesseral harmonic perturbations. Two averages can be considered – a single average over satellite's mean longitude λ and a second average over the other body's mean longitude λ^{O}. First, the single average over λ yields,

$$\delta\bar{\dot{\mathbf{x}}}^{O} \equiv \frac{1}{2\pi}\int_{-\pi}^{\pi}\sum_{q=-\infty}^{q=\infty}\sum_{t=-\infty}^{\infty}\mathbf{f}_{qt}^{O}(\boldsymbol{\alpha})\exp j\left[q\lambda - p\lambda^{O}\right]d\lambda = \frac{1}{\pi}\sum_{p=-\infty}^{\infty}\mathbf{f}_{0t}^{O}(\boldsymbol{\alpha})\exp j\left[-p\lambda^{O}\right]. \qquad (25)$$

where noting that $\lambda^{O} = n^{O}(t)t + \lambda_{o}^{O}$, shows that the single average still results in a non-autonomous system. The numerical propagator will select a step size that depends on the remaining secular terms, long period terms, and those terms with significant frequencies that are integral multiples of $n^{O}(t)$. Often this will not significantly increase the selected step size to impractical values, however in cases where it is warranted a second average over λ^{O} can be performed with the following result,

$$\delta\bar{\bar{\dot{\mathbf{x}}}}^{O} \equiv \frac{1}{2\pi}\int_{\lambda_{o}^{O}-\pi}^{\lambda_{o}^{O}+\pi}\frac{1}{\pi}\sum_{p=-\infty}^{\infty}\mathbf{f}_{0t}^{O}(\boldsymbol{\alpha})\exp j\left[-p\lambda^{O}\right]d\lambda^{O} = \frac{1}{\pi^{2}}\mathbf{f}_{00}^{O}(\boldsymbol{\alpha}). \qquad (26)$$

This result contains only terms with long period or secular frequencies. Morbiter offers both the single average and the double average options for any other body that is included in the propagation.

Example: Consider the same low altitude lunar orbiter as presented earlier in Table 1 except now include the perturbations from the Earth and Sun. As an initial investigation both the Earth and Sun are modeled with two-body orbits with initial elements defined from DE421 at the J2000 epoch. Future studies will examine the impact on the numerical averaging for other body perturbers using different ephemeris models.

The *e*-ω phase space results are shown in Figure 4 for a 3-yr propagation of the numerically single averaged EOMs that include only the zonal perturbations (labeled 'Zonal Single Avg' – a repeat of the first example), the single averaged propagation that includes zonals and the Earth/Sun perturbations (labeled 'Single Avg'), the double average propagation with zonals and Earth/Sun perturbations where the Earth is double averaged and the Sun is single averaged (labeled 'Double Avg'), and the Monte propagation of the direct osculating EOMs (labeled 'Osculating'). The libration characteristic is clearly evident, but significantly different than the prior zonal-only case. Both the 'Single Avg' and 'Double Avg' cases capture the correct qualitative dynamics as compared to the 'Osculating' result.

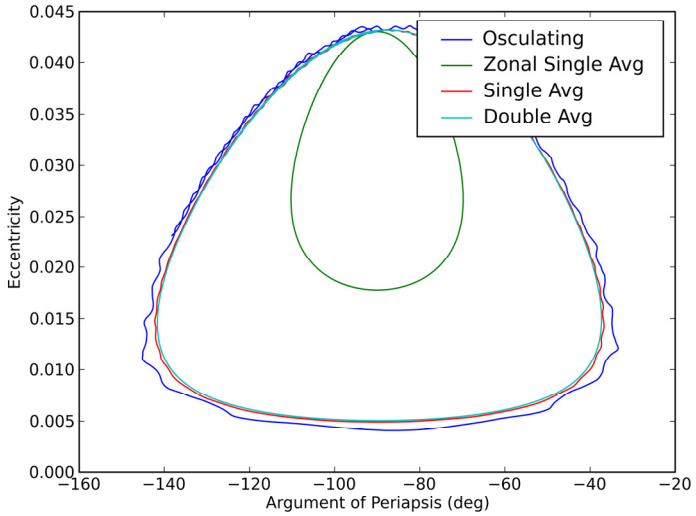

Figure 4: Argument of periapsis and eccentricity phase space of lunar orbiter that includes other body perturbations from the Sun and Earth.

Tabular results of the propagation performance are presented in Table 7. The results illustrate the inclusion of the other body perturbations significantly increases the number of required function calls for both the single average and double average cases as compared to the zonals-only. However, relative to the osculating results the averaged solutions are more efficient. The results also indicate that a double average for this example is not warranted relative to the single average case.

Table 7: Comparison of numerically single/double averaged EOMs 3-yr propagation to osculating EOMs

	Zonal-Only Single Average Gauss Fixed Order 64	**Zonals, Earth, and Sun Single Average Gauss Fixed** Order 64	**Zonals, Earth, and Sun Double Average Gauss Fixed** Order 64	**Osculating Monte**
Mean Step Size (# orbital periods)	140	8	58.8	0.004
# of Function Calls	12096	221,632	1,942,720	6,549,598
'Potential' Speed-Improvement Factor (osculating/mean function calls)	552.8	29.6	3.4	1

Drag and Solar Radiation Pressure Perturbations

Both of these perturbations are autonomous, hence the numerical averaging procedure that was previously defined for the zonal harmonics applies directly. Morbiter is capable performing this average, however work remains in adding the 2nd order drag/zonal harmonic coupling, and

making sure the averages are done only for those segments that are in the atmosphere and/or not being occulted by the central body. A detailed examination of the drag and solar radiation pressure perturbations will be presented in a future paper.

CONCLUSIONS

This study presented algorithms, methods, and results for numerically averaging two-body perturbed equations of motion to perturbations resulting from non-spherical gravity harmonics and other bodies. Perturbations for drag and solar radiation pressure can also be numerically averaged; however results for these will be presented in a future work. The results have shown that the numerically averaged propagations are more efficient then their osculating counterparts in capturing secular and long period motions. The numerical averaging technique correctly models these secular and long period motions, which has been ascertained via comparisons to osculating solutions from JPL's Monte software and to results from JPL's legacy semi-analytic software POLOP. It is also hypothesized that a future optimized and compiled language version of Morbiter will perform at least as well or better than the legacy semi-analytic technique. Future work will also focus on developing a numerical technique to determine the near identity transformation for converting between osculating and mean elements.

ACKNOWLEDGEMENTS

This work was carried out in part at the Jet Propulsion Laboratory, California Institute of Technology, under contract with the National Aeronautics and Space Administration.

APPENDIX: DIRECT EQUINOCTAL ELEMENTS AND PARTIALS

The direct equinoctial elements as functions of the classical elements $\{a, e, i, \Omega, \omega, M\}$ can be defined as,

$$\begin{aligned} a &\equiv a, \\ h &\equiv e\sin(\omega+\Omega), \\ k &\equiv e\cos(\omega+\Omega), \\ p &\equiv \tan\left(\frac{i}{2}\right)\sin\Omega, \\ q &\equiv \tan\left(\frac{i}{2}\right)\cos\Omega, \\ \lambda &\equiv M+\omega+\Omega. \end{aligned} \tag{27}$$

Some intermediate quantities are now defined. The equinoctial reference frame is composed of three orthogonal unit vectors $\{\mathbf{f}, \mathbf{g}, \mathbf{w}\}$ where,

1. $\mathbf{f}$ and $\mathbf{g}$ are in the satellite orbit plane,
2. $\mathbf{w}$ is along the orbit normal,
3. The angle between $\mathbf{f}$ and the ascending node is equal to the longitude of the ascending node Ω.

Using these properties the unit vectors $\{\mathbf{f}, \mathbf{g}, \mathbf{w}\}$ are obtained using,

$$\mathbf{f} = \frac{1}{1+p^2+q^2}\begin{bmatrix} 1-p^2+q^2 \\ 2pq \\ -2p \end{bmatrix},$$
$$\mathbf{g} = \frac{1}{1+p^2+q^2}\begin{bmatrix} 2pq \\ 1+p^2-q^2 \\ 2q \end{bmatrix}, \tag{28}$$
$$\mathbf{w} = \frac{1}{1+p^2+q^2}\begin{bmatrix} 2p \\ -2q \\ 1-p^2-q^2 \end{bmatrix}.$$

From the position $\mathbf{r}$ and velocity $\dot{\mathbf{r}}$ vectors the following components $\left\{X, Y, \dot{X}, \dot{Y}\right\}$ can be computed,

$$\begin{aligned} \mathbf{r} &\equiv X\mathbf{f} + Y\mathbf{g} \\ \dot{\mathbf{r}} &\equiv \dot{X}\mathbf{f} + \dot{Y}\mathbf{g} \end{aligned} \quad \rightarrow \quad \begin{aligned} X &= \mathbf{r}\bullet\mathbf{f}, Y = \mathbf{r}\bullet\mathbf{g} \\ \dot{X} &= \mathbf{r}\bullet\mathbf{f}, \dot{Y} = \mathbf{r}\bullet\mathbf{g} \end{aligned} . \tag{29}$$

Finally the partials identified in Gauss' Eqs. (6) are,

$$\begin{aligned}
\frac{\partial a}{\partial \dot{\mathbf{r}}} &= \frac{2a^2\dot{\mathbf{r}}}{\mu}, \\
\frac{\partial h}{\partial \dot{\mathbf{r}}} &= \frac{\left(2\dot{X}Y - X\dot{Y}\right)\mathbf{f} - X\dot{X}\mathbf{g}}{\mu} + \frac{k\left(qY - pX\right)\mathbf{w}}{AB}, \\
\frac{\partial k}{\partial \dot{\mathbf{r}}} &= \frac{\left(2X\dot{Y} - \dot{X}Y\right)\mathbf{f} - Y\dot{Y}\mathbf{g}}{\mu} - \frac{h\left(qY - pX\right)\mathbf{w}}{AB}, \\
\frac{\partial p}{\partial \dot{\mathbf{r}}} &= \frac{CY\mathbf{w}}{2AB}, \\
\frac{\partial q}{\partial \dot{\mathbf{r}}} &= \frac{CX\mathbf{w}}{2AB}, \\
\frac{\partial \lambda}{\partial \dot{\mathbf{r}}} &= -\frac{2\mathbf{r}}{A} + \frac{k\dfrac{\partial h}{\partial \dot{\mathbf{r}}} - h\dfrac{\partial k}{\partial \dot{\mathbf{r}}}}{1+B} + \frac{\left(qY - pX\right)\mathbf{w}}{A},
\end{aligned} \tag{30}$$

Where it should be noted that the expression for $\partial a/\partial \dot{\mathbf{r}}$ in Danielson [14] is incorrect, the correct version is shown in Eq. (30)

REFERENCES

1. Cefola, P., A.C. Long, and G. Holloway, Jr., *The Long-Term Prediction of Artificial Satellite Orbits*, in *12th Aerospace Sciences Meeting*. 1974, AIAA: Washington, D. C. p. 33.

2. Cefola, P., et al. *A semianalytical satellite theory for weak time-dependent perturbations*. in *Flight Mechanics/Estimation Theory Symposium*. 1980.
3. McClain, W.D., *A recursively formulated first-order semianalytic artificial satellite theory based on the generalized method of averaging. Volume 1: The generalized method of averaging applied to the artificial satellite problem*, in *Unknown*. 1977, Computer Sciences Corporation.
4. McClain, W.D., *A recursively formulated first-order semianalytic artificial satellite theory based on the generalized method of averaging. Volume 2: The explicit development of the first-order averaged equations of motion and for the nonspherical gravitational and nonresonant third-body perturbations*. 1978, Computer Sciences Corporation.
5. McClain, W.D., A.C. Long, and L.W. Early. *Development and evaluation of a hybrid averaged orbit generator*. in *AIAA, Astrodynamics Conference*. 1978.
6. Kwok, J.H. *Long-term orbit prediction for the Venus Radar Mapper Mission using an averaging method*. in *AAS/AIAA Astrodynamics Conference*. 1984.
7. Kwok, J.H., *The implementation of two satellite programs in a microcomputer environment*, in *AIAA/AAS Astrodynamics Conference*. 1986: Williamsburg, VA.
8. Uphoff, C., *Numerical averaging in orbit prediction.* AIAA Journal, 1973. **11**: p. 1512-1516.
9. Lutzky, D. and C. Uphoff. *Short-periodic variations and second-order numerical averaging*. in *AIAA, Aerospace Sciences Meeting*. 1975.
10. Genz, A. and R. Cools, *An adaptive numerical cubature algorithm for simplices.* ACM Trans. Math. Softw., 2003. **29**(3): p. 297-308.
11. Cools, R. and A. Haegemans, *Algorithm 824: CUBPACK: a package for automatic cubature; framework description.* ACM Trans. Math. Softw., 2003. **29**(3): p. 287-296.
12. Sanders, J., F. Verhulst, and J. Murdock, *Averaging Methods in Nonlinear Dynamical Systems*. 2nd ed. Applied Mathematical Sciences, ed. S.S. Antman, J.E. Marsden, and L. Sirovich. 2007: Springer.
13. Smyth, G.K., *Numerical Integration*, in *Encyclopedia of Biostatistics*. 1998. p. 3088--3095.
14. Danielson, D.A., B. Neta, and L.W. Early, *Semi-Analytic Satellite Theory (SST): Mathematical Algorithms*. 1994, Naval Postgraduate School. p. 106.
15. Cefola, P. *A recursive formulation for the tesseral disturbing function in equinoctial variables*. in *American Institute of Aeronautics and Astronautics and American Astronautical Society, Astrodynamics Conference, San Diego, Calif., Aug. 18-20, 1976, AIAA 12 p. DARPA-sponsored research;*. 1976.
16. Lichtenberg, A.J. and M.A. Lieberman, *Regular and Chaotic Dynamics*. 2nd ed. Applied Mathematical Sciences. 1992: Springer.